第 21 卷 第 2 期
2004 年 6 月

原子核物理评论
Nuclear Physics Review

Vol. 21, No. 2
June, 2004

Article ID: 1007—4627(2004)02—0130—07

Reflection Asymmetric Shell Model for Octupole Nuclei*

CHEN Yong-shou

(*China Institute of Atomic Energy, Beijing* 102413, *China*)

(*Institute of Theoretical Physics, Chinese Academy of Seiences, Beijing* 100080, *China*)

Abstract: The reflection asymmetric shell model approach has been developed for the description of octupole deformed nuclei. The $Q \cdot Q$ forces of quadrupole, octupole and hexadecapole as well as the monopole and quadrupole pairings are included in the Hamiltonian. The shell model space is spanned by a selected set of the projected axial and octupole Nilsson + BSC basis. The general features of experimental octupole rotational bands can be reproduced and interpreted by the present model. The experimental super-deformed band states in ^{190,194}Hg are well reproduced by the present calculations, which provide theoretical support to the possible experimental evidence for the discovery of the octupole super-deformed rotational bands.

Key words: octupole; shell model; super-deformation

CLC number: O571 **Document code**: A

1 Introduction

It is my great pleasure to speak at the symposium on the frontiers of theoretical physics honoring Prof. Wu Shishu at occasion of his 80th birth day. I shall address some of the recent developments of the shell model description of octupole deformed nuclei. The shell model provides a fundamental way to deal with nuclear many body problem. Prof. Wu made variety of important contributions to the study of nuclear many body problem. As an example, he studied the single particle potential based on the mass operator, $U_{\alpha\beta}=M_{\alpha\beta}(\varepsilon_\beta)$, by using the Green's function method he proved that the discrete eigenvalue must be real although U is non-hermite and the equation $\varepsilon_\beta=\pm(E_{n\beta}(A\pm 1)-E_0(A))$ must be exactly full filled. Where $E_0(A)$ is the ground state energy of the shell closure nucleus A and $E_{n\beta}(A\pm 1)$ are the energies of $n\beta$th states in the neighbour $A\pm 1$ nuclei. This allows us to choice a good U by fitting to the experimental s. p. energy spectrum. This method has been widely used in the shell model studies, including the present work, but the validity for the method may be found from Prof. Wu's works, see, for example, Ref. [1].

The study of nuclei with exotic shapes is one of the most vital fields in modern nuclear structure physics. A nucleus characteristic of reflation asymmetric intrinsic shape is often referred as octupole deformed. The sequence of rotational states with alternating odd and even spin-parity, I^+, $(I+1)^-$, $(I+2)^+$, $\cdots$, here I is even integer number, was observed in ^{222}Ra[2], as an example. These band structures are analogous to those of asymmetric molecules such as $H^{35}Cl$ and may be expected for nuclei with octupole deformation, see Fig. 1.

Received date: 9 Feb. 2004; **Corrected date**: 17 Mar. 2004

* **Foundation item**: National Natural Science Foundation of China (10075078, 19935030, 10047001); Major State Research Development Program of China (G20000774)

Biography: ChenYongshou(1939—), male(Han Nationality), Sichuan Luzhou, Professor, working on nuclear structure and nuclear astrophysics.

The striking behavior of the octupole bands highlights the nuclear reflection asymmetry and has attracted much interest over the years. In the recent years special interest attaches to the super-deformed (SD) octupole nuclei with a ratio of 2 : 1 for the long to short axis and a mass asymmetry. This exotic shape has not yet been identified experimentally although more than a hundred SD bands were measured. The present study provides theoretical support for the possible experimental evidence for the discovery of SD octupole nuclei.

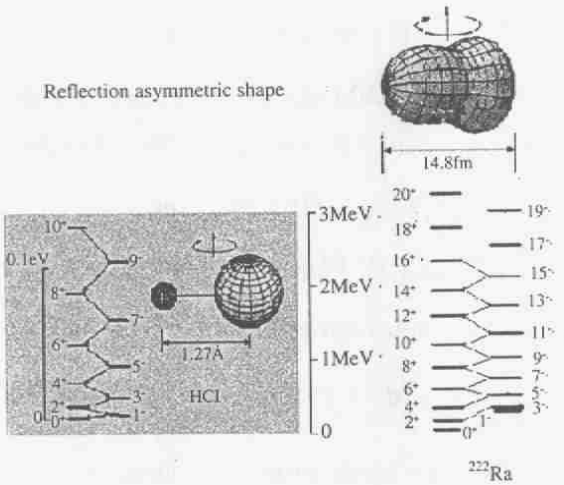

Fig. 1 The low-lying spectra of the $H^{35}Cl$ molecule and ^{226}Ra. The similarity is seen for the two spectra, indicating reflation asymmetry shape of the nucleus. The sketched octupole shapes are shown at the top of the figure.

2 Brief Description of RASM

In the reflection asymmetric shell model (RASM) approach[3], we first break both the quadrupole and octupole symmetries and then recover them by carrying out the simultaneous angular momentum and parity projections from a chosen set of Nilsson + BCS states near the Fermi surfaces. The projected states are then used to diagonalize the spherical shell model Hamiltonian. The approach follows the basic philosophy of the standard shell model, and the only difference is that, in the RASM, the deformed basis is employed rather than the spherical one. With such projected basis the shell model truncation of the many-body basis becomes in practice efficient so that the shell model calculation can be performed even for heavy and superdeformed nuclei. In contrast, the standard (spherical) shell model description for heavy nuclei is almost impossible even with the huge progress in the modern computer technology. We will show that the shell model space spanned by the states of only three major shells for protons and neutrons respectively is large enough for the RASM calculation of the low- lying octupole bands in heavy octupole deformed nuclei, and that calculated results are in a good agreement with the experimental data.

The shell model Hamiltonian considered in the present work involves a large number of nucleons moving in a spherical Nilsson potential and an interaction of separable multipole $Q \cdot Q$ plus monopole pairing plus quardrupole pairing,

$$H = H_0 - \frac{1}{2}\sum_{\lambda=2}^{4}\chi\lambda\sum_{\mu=-\lambda}^{\lambda}Q^{\dagger}_{\lambda\mu}Q_{\lambda\mu} - G_0 P^{\dagger}_{00}P_{00} - G_2\sum_{\mu=-2}^{2}P^{\dagger}_{2\mu}P_{2\mu}\ , \qquad (1)$$

where H_0 is the spherical modified harmonic-oscillator single particle Hamiltonian, and the operators Q and P are expressed as

$$Q_{\lambda\mu} = \sum_{\alpha,\beta}\langle\alpha\mid\rho^2 Y_{\lambda\mu}\mid\beta\rangle\ c^{\dagger}_{\alpha}c_{\beta}\ , \qquad (2)$$

$$P^{\dagger}_{00} = \frac{1}{2}\sum_{\alpha}c^{\dagger}_{\alpha}c^{\dagger}_{\bar{\alpha}}, \qquad (3)$$

$$P^{\dagger}_{2\mu} = \frac{1}{2}\sum_{\alpha,\beta}\langle\alpha\mid\rho^2 Y_{2\mu}\mid\beta\rangle\ c^{\dagger}_{\alpha}c^{\dagger}_{\bar{\beta}}. \qquad (4)$$

Where, the eigenstates of a single particle moving in the spherical Nilsson potential can be labelled by the quantum numbers $\alpha=nljm$ where n is the radial quantum number, l is the orbital angular momentum, j is the total angular momentum, and m is the component of j on the axis of quantization, and $\bar{\alpha}$ denotes the time-reversed state of α.

The coupling constants of the $Q_\lambda \cdot Q_\lambda$ forces, $\chi\lambda$ in Eq. (1), can be determined in consistent to

the deformations,

$$\chi_{2,\tau\tau'}=\frac{\frac{2}{3}\sqrt{\frac{4\pi}{5}}\varepsilon_2\hbar\omega_\tau\hbar\omega_{\tau'}}{\hbar\omega_n\langle Q_{20}\rangle_n+\hbar\omega_p\langle Q_{20}\rangle_p},$$

$$\chi_{3,\tau\tau'}=\frac{-\sqrt{\frac{4\pi}{7}}\varepsilon_3\hbar\omega_\tau\hbar\omega_{\tau'}}{\hbar\omega_n\langle Q_{30}\rangle_n+\hbar\omega_p\langle Q_{30}\rangle_p},$$

$$\chi_{4,\tau\tau'}=\frac{-\sqrt{\frac{4\pi}{9}}\varepsilon_4\hbar\omega_\tau\hbar\omega_{\tau'}}{\hbar\omega_n\langle Q_{40}\rangle_n+\hbar\omega_p\langle Q_{40}\rangle_p}, \quad (5)$$

where $\langle\cdots\rangle$ denotes the expectation value with respect to the BCS vacuum state, $\tau(\tau')$ refers to neutrons or protons.

The standard expression of the monopole pairing strength is used,

$$G_0=\frac{g_1\mp g_2(N-Z)/A}{A}, \quad (6)$$

where $-(+)$ stands for the neutrons (protons), and the standard pairing parameters $g_1=21.24$ and $g_2=13.86$ MeV is usually taken and a reduction factor may be used in some cases. For Ra isotopes, the pairing parameters with a reduction factor of about 0.82 are taken, and the quadrupole pairing strength is set to zero. In the present calculation for SD nuclei, the pairing parameters with a reduction factor of 0.8 are taken. By considering the enhancement of the quadrupole pairing in SD nuclei, the quadrupole pairing strength is set to $G_2=0.28\,G_0$, which is larger than that for normal deformed nuclei where the multiplied factor is usually 0.16 or zero.

In the construction of the Nilsson + BCS basis the usual BCS approximation is used to treat the (static) pairing correlations, and then the intrinsic deformed states are labeled by the quasiparticle configurations κ. We consider a set of intrinsic states $\{|\Phi_\kappa\rangle\}$ with the quadrupole and octupole deformations, which are not the eigenstates of angular momentum and parity. A trial wave function can be constructed as the superposition of oriented in space and the "left-right" to "right-left" reflected intrinsic wave functions,

$$|\Psi\rangle=\sum_\kappa\int d\Omega\,[F_{1\kappa}(\Omega)+F_{2\kappa}(\Omega)\hat{P}]\hat{R}(\Omega)\,|\Phi_\kappa\rangle, \quad (7)$$

where $R(\Omega)$ is the rotational operator, Ω represents a set of Euler angles, $\hat{P}$ is the parity operator, and it is obvious that $[\hat{P},\hat{R}(\Omega)]=0$. Note that the configuration mixing is included in Eq. (7), which is necessary in order to deal with interaction between unperturbed bands. The coefficient $F_{1\kappa}(\Omega)$ and $F_{2\kappa}(\Omega)$ functions can be determined by the variational procedure. By solving the variational equation

$$\delta\langle\Psi|H|\Psi\rangle-E\delta\langle\Psi|\Psi\rangle=0, \quad (8)$$

we obtain the RASM eigenvalue equation with the eigenvalue E^{Ip} for a given spin I and parity p,

$$\sum_{K\kappa}\{\langle\Phi_{\kappa'}|HP^pP^I_{K'K}|\Phi_\kappa\rangle-E^{Ip}\langle\Phi_{\kappa'}|P^pP^I_{K'K}|\Phi_\kappa\rangle\}F^{Ip}_{MK\kappa}=0, \quad (9)$$

with the normalization condition

$$\sum_{K'\kappa'K\kappa}F^{Ip*}_{MK'\kappa'}\langle\Phi_{\kappa'}|P^pP^I_{K'K}|\Phi_\kappa\rangle F^{Ip}_{MK\kappa}=1, \quad (10)$$

where P^p is the parity projection operator

$$P^p=\frac{1}{2}(1+p\hat{P}), \quad (11)$$

with $p=\pm1$, and P^I_{MK} is the angular momentum projection operator

$$P^I_{MK}=\frac{2I+1}{8\pi^2}\int d\Omega\,D^I_{MK}(\Omega)\hat{R}(\Omega). \quad (12)$$

It is obvious that Eq. (4) is valid for any nuclear shape. In the present study we consider reflection asymmetric shape of axially symmetry, and thus the angular momentum projection operation reduces to the one dimensional integration. The Eq. (9) is in fact a diagonalization of the Hamiltonian within the shell model space spanned by $P^pP^I_{MK}|\Phi_\kappa\rangle$, the simultaneously parity and angular momentum projected states from the intrinsic BCS quasiparticle states. The quasiparticle configurations employed in the present calculation include the vacuum $|0\rangle$, two q. p. neutrons $a^\dagger_{\mu1}a^\dagger_{\mu2}|0\rangle$, two q. p. protons $a^\dagger_{\pi1}a^\dagger_{\pi2}|0\rangle$ and four quasiparticle

states $a^{\dagger}_{\mu 1}\, a^{\dagger}_{\mu 2}\, a^{\dagger}_{\pi 1} a^{\dagger}_{\pi 2}\,|0\rangle$. Where μ's (π's) denote the neutron (proton) Nilsson quantum numbers.

3 Octupole Bands in Ra isotopes

First we shall apply the model to well defined octupole nuclei, Ra isotopes. The three major shells of $N=5$, 6, 7 for neutrons and $N=4$, 5, 6 for protons are included for the calculations. The calculated octupole bands, energy versus spin, up to spin 26 are shown as solid lines in Fig. 2. The theoretical bands are compared with the experimental positive parity and even spin band with $K^{\pi}=0^{+}$ (solid circles) and negative parity odd spin band with $K^{\pi}=0^{-}$ (open circles). It is seen that the agreement between experiment and theory is remarkable. One of striking features for octupole bands is of presence of the significant parity splitting at low spins. The parity splitting measures to the extent to which the odd-spin negative parity level of spin I has an excitation energy located

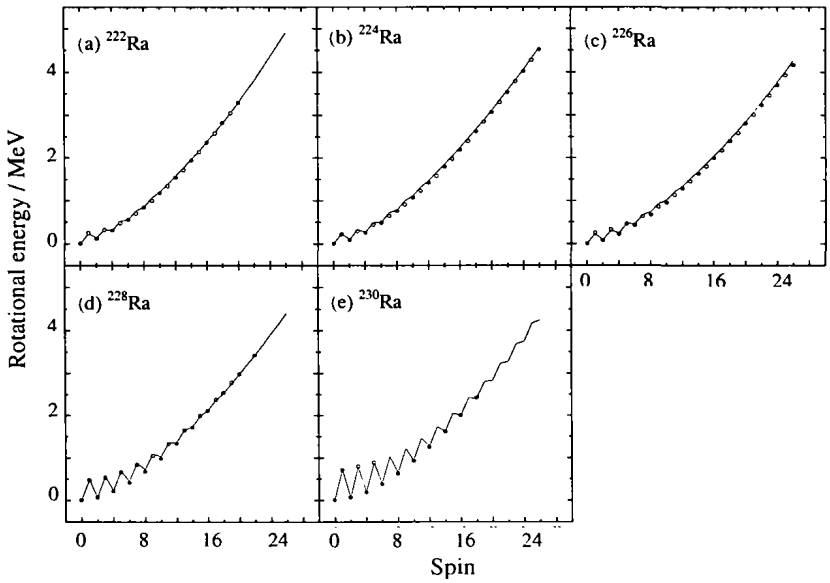

Fig. 2 The calculated yrast rotational bands (solid lines), energy versus spin, for $^{222-230}$Ra are compared with the experimental data (open circles for negative and solid circles for positive parities), taken from Ref. [5].

higher than the average of those of the two neighboring even-spin positive parity states with respective spins $I-1$ and $I+1$. This quantity is one of the unique features of octupole modes, and has attracted much interest over the years. The parity splitting of rotational octupole bands may be quenched due to fast rotation and there usually exist a critical spin I_c at which parity splitting vanishes and the negative and positive parity states become interleaved according to the energy formula $E_I \sim I(I+1)$. An other striking feature of octupole bands is the absence of the sharp band crossing. This feature is also reproduced by the RASM calculations. Even a small octupole deformation will significantly mix the high-j intruder shells with other valence orbitals. The rotational strength is then distributed over the valence nucleons, and thus back-bends are generally smothed out. This mechanism associated only with octupole deformation is included in both the cranking and angular momentum projection pictures in the application of the mean field theory.

As discussed above, there are four striking features of octupole bands which are distinct from the normal rotational bands: the specific sequence of states 0^{+}, 1^{-}, 2^{+}, 3^{-}, $\cdots$, the significant parity splitting at low spins, the quenching of the parity splitting by rotation and the absence of the sharp band crossing. All these features characteristic of rotation of octupole deformed nuclei can be ex-

plained and reproduced within the frame work of the RASM.

4 Possible Evidence for Octupole SD Nuclei

The large γ-ray spectrometer arrays GAMMASPHERE and EUROBALL have made it possible to establish the linking transitions from SD to normal-deformed (ND) states, e. g., in ^{194}Hg. The energies, spins and parities of the excited SD band 3 and the yrast SD band 1 in ^{194}Hg were determined experimentally and band 3 is proposed to be a collective $K^\pi=2^-$ octupole vibrational band [4] rather than a 2-qp neutron configuration. This experimental data supports the cranking RPA calculations which result in that the lowest excited states in the SD minimum are octupole vibrations in $^{190-194}$Hg[5]. In the present work an alternative explanation is given, the yrast positive parity SD bands 1 in ^{190,194}Hg and the excited negative parity SD bands 3 and 2 observed in ^{194}Hg and ^{190}Hg, respectively, are described in terms of the parity partner octupole bands, namely, band 1 with $K^\pi=0^+$ and bands 3 and 2 with $K^\pi=0^-$.

The RASM equation has been solved for the SD states in ^{190,194}Hg up to spin 50. In the calculation of the Nilsson + BCS basis, the octupole Nilsson potential has been solved with three major shells $N=5$, 6, 7(4, 5, 6) for neutrons (protons), using the standard Nilsson parameters κ and μ taken from Ref. [6]. The lowest octupole SD bands for ^{194}Hg, namely the positive parity Yrast SD band with $K^\pi=0^+$ and the negative parity excited SD band with $K^\pi=0^-$, calculated with deformation parameters $\varepsilon_2=0.428$, $\varepsilon_3=0.062$ and $\varepsilon_4=-0.004$ are shown and compared with experimental SD bands 1 and 3 in Fig. 3. It is seen from Fig. 3 that both the experimental negative parity excited SD band (open circles) and the positive parity Yrast SD band (solid circles) are well reproduced by the present calculation (solid lines), including the energies, spins and parity. The same lowest octupole SD bands but for ^{190}Hg, calculated with deformation parameters $\varepsilon_2=0.445$, $\varepsilon_3=0.058$ and $\varepsilon_4=-0.004$ are shown and compared with experimental SD bands 1 and 2 in Fig. 4. It should be noticed that the spins of the experimental SD bands in ^{190}Hg have not been assigned experimentally. However, the excitation energy of band 2 relative to the SD Yrast band 1 has been determined firmly by the observation of the four discrete γ-rays linking SD band 2 and band 1, see Ref. [7] and references therein. The present calculation yields the assignments of spins as shown in Fig. 4 by the best fit for experimental γ-ray energies of the inband and interband transitions, which turns out to be in coincidence with the tentative spin assignments of Ref. [8]. It is seen from Fig. 4 that both the experimental negative parity excited SD band (open circles) and the positive parity Yrast SD band (solid circles) are well reproduced by the present calculation (solid lines), including the energies, spins and parity.

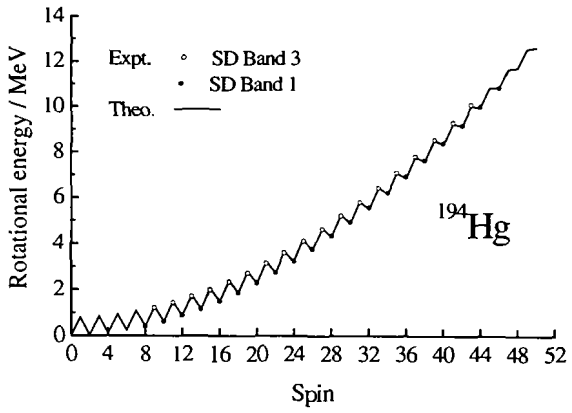

Fig. 3 The calculated lowest SD octupole rotational bands (solid lines), energy versus spin, are plotted and compared with experimental SD bands 1 (solid circles) and 3 (open circles) in ^{194}Hg [4]. The energy of the ground SD state is set to zero.

It is seen from Figs. 3 and 4 that both the experimental parity splitting and its rotational quenching have been well reproduced by the present calculations. It should be noticed that although the parity splitting at one spin point can be repro-

duced by adjusting the octupole coupling constant χ_3 through the change of ϵ_3 deformation, the good agreement between the theory and experiment over the whole observed spins is not trivial at all. The calculated excitation energy of the band head 1^- of SD band 3 above the SD vacuum state 0^+ in ^{194}Hg is 0.796 MeV, which is in extremely good agreement with the experimentally extrapolated excitation energy of $\sim$ 0.8 MeV at zero frequency in Ref. [3]. The calculated same quantity but for ^{190}Hg is 1.097 MeV for which no experimental data is available.

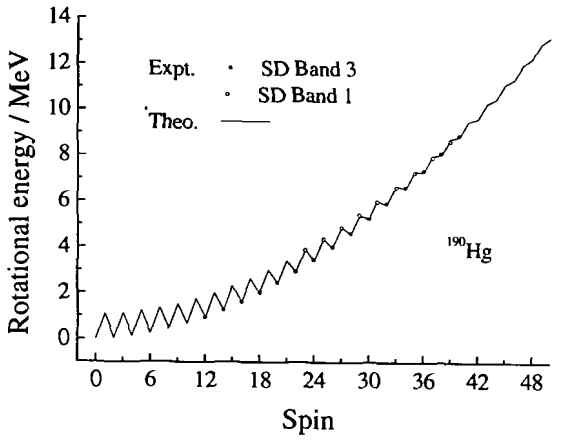

Fig4 The calculated lowest SD octupole rotational bands (solid lines), energy versus spin, are plotted and compared with experimental SD bands 1 (solid circles) and 2 (open circles) in ^{190}Hg [7]. The energy of the ground SD state is set to zero.

It is generally true that a large parity splitting may be associated with the octupole vibrational mode. However, a small parity splitting may imply the occurrence of the static octupole deformation. The observed yrast spectra for well octupole deformed nuclei, e. g., $^{220-230}$Ra, show considerable parity splitting at low spins, 200—500 keV, and nearly zero parity splitting at high spins, see Ref. [2]. Therefore, it may be reasonable to explain the nature of these octupole SD bands such that the considerable parity splitting at low spins indicates the soft octupole rotation and the rather small parity splitting at higher spins, due to the rotational quenching, implies octupole super-deformation. The rather large parity splitting presented in ^{194}Hg may indicate that the nature of SD band 3 is transitional from the vibrational to rotational modes. However, the SD band 2 in ^{190}Hg behaves differently that the rotational quenching of the parity splitting is much stronger than that for ^{194}Hg, so that the parity splitting reduces to 150 keV around spin 39, which is similar to the typical value at low spins in the octupole deformed Ra nuclei. This fact draws heavy on the suggestion that the SD octupole rotation, and thus an octupole super-deformation, soft may be, rather than a vibration around non-octupole shape, may occur at high spins in ^{190}Hg. The proton $(2f_{7/2}, 1i_{13/2})$ and neutron $(2g_{9/2}, 1j_{15/2})$ orbital pairs, which lead to strong couplings of the octupole Y_{30} term, come close to the Fermi surfaces in the Hg-region at large deformation $\epsilon_2 \sim 0.45$, providing the microscopic basis for the presence of octupole SD modes. we point out that it is just the same orbital pairs to provide the strong octupole couplings in the Ra region but at a normal deformation, $\epsilon_2 \approx 0.1$. In other words, the SD octupole mode in the Hg region and the ND octupole mode in the Ra region have the same microscopic origin. The strong quenching of the parity splitting in ^{190}Hg may be understood by analyzing the octupole couplings of obital pairs. The high-j and low-K components of the neutron $(2g_{9/2}, 1j_{15/2})$ orbital pairs, e. g., ([642]3/2, [761]3/2) Nilsson-orbital pair, come close to the neutron Fermi surface, $N=110$, in ^{190}Hg, which generate a strong octupole coupling in the one hand and response strongly to the fast rotation in the other hand, and consequently, the rotational quenching of parity splitting becomes stronger. Whereas such high-j and low-K components are less close to the neutron Fermi surface, $N=114$, in ^{194}Hg and thus only a slightly quenching of the parity splitting appears with increasing spin up to 50. The validity of this explanation is further proved by the fact that the rotational quenching of the parity splitting was found to be weak too in

^{196}Pb with $N=114$.

5 Summary

In summary, the reflection asymmetric shell model approach has been introduced to describe the SD band states in ^{190,194}Hg for a rigorous test of theory, e. g. , of predictions of low-lying octupole collectivity in SD nuclei, by taking the advantage of the experimentally determined spins, parity and excitation energies of the excited SD bands. In the RASM approach the simultaneous angular momentum and parity projections are carried out from a set of the intrinsic octupole deformed Nilsson + BCS states and the projected states with good parity and angular momentum are employed to form the basis in which the shell model Hamiltonian is diagonalized. The RASM equation has been solved for the SD states in ^{190,194}Hg up to spin 50. The experimental excited negative parity odd-spin SD bands, band 3 in ^{194}Hg and band 2 in ^{190}Hg, and together with their positive parity even-spin yrast SD bands are well reproduced by the present calculations, and interpreted as the transitional octupole SD bands having $K^{\pi}=0^{-}$ (excited) and $K^{\pi}=0^{+}$ (Yrast). The picture of the octupole SD bands described in this paper draws heavy on the suggestion that the SD octupole rotation, thus the octupole superdeformation, may occur at high spins in ^{190}Hg. The interesting features of transitional octupole SD bands that are briefly sketched in the present work are the subjects of future studies.

References:

[1] Wu Shishu. Scientia Sinina, 1981, **24**.

[2] Cocks J F C, Hawcroft D, Amzal N, *et al*. Nucl Phys, 1999, **A645**: 61.

[3] Chen Y S, Gao Z C. Phys Rev, 2001, **C63**: 014314.

[4] Hackman G, Khoo T L, Carpenter M P, *et al*. Phys Rev Lett, 1997, **79**: 4 100.

[5] Nakatsukasa T, Matsuyanagi K, Mizutori S, *et al*. Phys Rev, 1996, **C53**: 2 213.

[6] Bengsson T, Ragnarsson I. Nucl Phys, 1985, **A436**: 14.

[7] Korichi A, Wilson A N, Hannachi F, *et al*. Phys Rev Lett, 2001, **86**: 2 746.

[8] Wilson A N, Timar J, Sharpey-Schafer J F, *et al*. Phys Rev, 1996, **C54**: 559.

八极形变核的反射不对称壳模型描述*

陈永寿

(中国原子能科学研究院，北京 102413)

(中国科学院理论物理研究所，北京 100080)

摘 要：发展反射不对称壳模型，描述八极形变核. 哈密尔顿量包含了四极、八极和十六极多极力，单极和四极对力. 壳模型空间由八极形变轴对称 Nilsson 势加 BCS 的投影基矢构成. 理论模型再现了和解释了实验八极转动带的基本特性. 理论计算很好地再现了^{190,194}Hg 的超形变转动带实验谱，从而为八极超形变转动带的可能的实验证据提供了理论支持.

关 键 词：八极转动带；壳模型；超形变

* **基金项目**：国家自然科学基金资助项目(10075078, 19935030, 10047001)；国家重点基础研究发展计划资助项目(G20000774)